

Intricate Hydrogen-Bonded Networks: Binary and Ternary Combinations of Uracil, PTCDI, and Melamine

Jules A. Gardener,*† Olga Y. Shvarova, G. Andrew D. Briggs, and Martin R. Castell*

Department of Materials, University of Oxford, Oxford, OX1 3PH, United Kingdom

Received: November 29, 2009; Revised Manuscript Received: January 31, 2010

We report the formation of two- and three-component porous supramolecular networks from combinations of uracil, PTCDI, and melamine. The structures, which are formed on Au(111) in ultra-high vacuum (UHV) and studied by scanning tunneling microscopy (STM), are stabilized by hydrogen bonds. We show that two bimolecular networks comprising uracil and PTCDI can be formed, one of which contains two pore geometries and is composed of 28 molecules per unit cell. In addition, we observe two different ordered structures from mixtures of melamine and uracil. By combining all three of these species, we demonstrate the formation of a single ternary structure that contains 33 molecules per unit cell. Our results demonstrate the capacity of hydrogen bonding to produce highly complex structures, and open up the possibility of forming a wide range of new structures from combinations of nucleic bases and other small organic molecules.

Introduction

A range of porous two-dimensional supramolecular networks can be constructed on surfaces through careful choice of the molecular components and the substrate.¹ This is primarily achieved through hydrogen bonding, metal–organic co-ordination, van der Waals interactions, or covalent bonding. Here, we concentrate on combinations of organic molecules with the capacity to form hydrogen bonds. Such an approach is advantageous since hydrogen bonds are highly directional, leading to ordered structures, but sufficiently weak to allow molecular diffusion on surfaces at room temperature. These properties can result in the formation of ordered molecular structures over large areas. Further, some of these networks may contain pores and can act as templates for the ordering of guest molecules such as fullerenes.^{2–9}

Some nucleic bases and other small organic molecules can form monomer porous two-dimensional structures stabilized by hydrogen bonding.^{10–14} However, a greater variety of networks can be generated through the combination of two complementary molecular species. For example, four different supramolecular networks of 3,4,9,10-perylenetetracarboxylic diimide (PTCDI) and 1,3,4-triazine-2,4,6-triamine (melamine) have been reported,^{2,6–8,15,16} of which three contain pores that act as absorption sites for guest molecules. Bimolecular networks generally have more complex unit cells than their monomer counterparts, and offer a wider range of pore sizes, geometries, and interpore separations. Recently, coronene-templated three-component networks have been reported, which are even larger and more intricate (we define intricacy in terms of the number of molecules per unit cell).^{17,18} However, these appear to show little capacity to host molecules other than coronene.

In this work, we have combined two different systems that are well-known to form hydrogen-bonded supramolecular networks: a nucleic base with PTCDI-melamine. The nucleic base that we have chosen is uracil, a molecule that forms planar

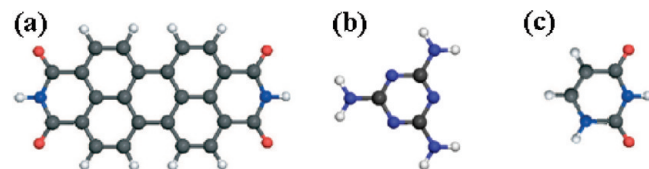


Figure 1. The molecular structures of (a) PTCDI, (b) melamine, and (c) uracil. Balls represent carbon (gray), oxygen (red), nitrogen (blue), and hydrogen (white) atoms.

hydrogen-bonded structures in two and three dimensions.^{19–21} The chemical structures of the three molecules studied are shown in Figure 1. Uracil is prochiral; when constrained to lie parallel to a surface, it can adopt one of two possible orientations and these have no mirror symmetry, giving rise to chirality. However, PTCDI and melamine are not chiral, even when constrained to two dimensions. Here, we deposit uracil, PTCDI, and melamine onto Au(111), by sublimation. Through the careful selection and postdeposition processing of the component molecules, we demonstrate the formation of ordered binary and ternary supramolecular networks, some of which have remarkably intricate unit cells.

Experimental Methods

All experiments were performed *in situ* under UHV conditions (base pressure of $\sim 1 \times 10^{-8}$ Pa). Au(111) films on mica (Agilent) were prepared by Ar^+ sputtering and annealing to ~ 600 °C, a procedure that produced large flat terraces displaying the characteristic $22 \times \sqrt{3}$ reconstruction. Melamine (Aldrich), PTCDI (TCI Europe), and uracil (Aldrich) were sublimed at typical rates of 8–15 ML/h (ML=monolayers), 0.6–0.8 ML/h, and 0.1–0.3 ML/h (unless otherwise stated), respectively, onto the Au substrates, which were held at room temperature. The samples were subjected to postdeposition annealing for 10–14 h; shorter anneals (typically a few hours) and lower temperatures resulted in less ordered structures. A JEOL JSTM4500S STM was used to obtain constant current images (bias applied to the sample) at room temperature, using electrochemically etched W tips. All images were processed with WSxM software.²²

* To whom correspondence should be addressed. gardener@fas.harvard.edu and martin.castell@materials.ox.ac.uk.

† Present address: Department of Physics, Harvard University, Cambridge, MA 02138.

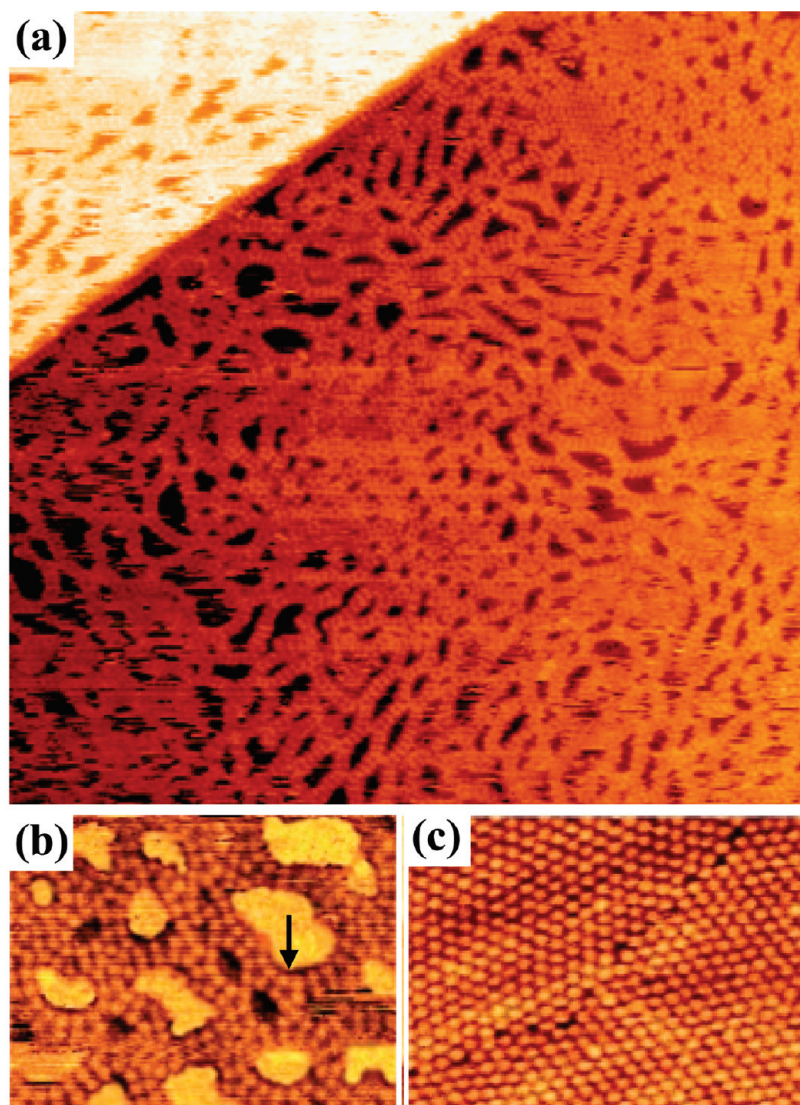


Figure 2. (a) Disordered chain-like structures of uracil ($V_s = +1.35$ V, $I_t = 0.07$ nA, $85\text{ nm} \times 85$ nm). (b) A higher resolution image of the chains, which are double rows of uracil molecules ($V_s = +1.44$ V, $I_t = 0.07$ nA, $16.0\text{ nm} \times 12.0$ nm). A black arrow highlights a pentagonal cluster of uracil. (c) A region of close-packed uracil ($V_s = -1.40$ V, $I_t = 0.10$ nA, $16.0\text{ nm} \times 12.0$ nm). Uracil was deposited at a rate of $0.9\text{--}1.0$ ML/h for all images shown in this figure.

Results and Discussion

First, we characterize the self-assembly of uracil after deposition onto a clean $22 \times \sqrt{3}$ reconstructed Au(111) film on mica. We observe two different structures, as shown in Figure 2. At moderately low coverages, chain-like features are formed, as shown in Figure 2a. These structures often form closed rings, but show no long-range ordering. High-resolution images, such as Figure 2b, show that the chains comprise double rows of uracil molecules, while pentagonal clusters are frequently observed where multiple chains join (for example, as indicated by an arrow in the figure). The uracil chains are similar to those formed by flat-lying cytosine or thymine on Au(111), stabilized by in-plane hydrogen bonds;^{23–25} any differences in molecular positioning within the chains are attributed to the nonequivalent hydrogen bonding sites of different nucleic bases. At higher molecular coverages we find close-packed regions (Figure 2c). In this arrangement, each uracil is generally surrounded by six other uracil molecules, again forming a hydrogen-bonded network.^{19,20}

New porous structures are observed after sequential deposition of $0.1\text{--}0.3$ ML of uracil then $0.3\text{--}0.4$ ML of PTCI at room

temperature, followed by annealing to ~ 85 °C for ~ 10 h, examples of which are shown in Figures 3 and 4. On average, these structures cover a combined total of 34% of the Au(111) surface, while some residual close-packed PTCI patches remain (any excess uracil is likely to have desorbed from the surface during annealing). The differences in size, shape, and electronic structure of PTCI and uracil allows them to be distinguished in the STM images; PTCI appear as bright rectangles, while uracil molecules are seen as smaller, round features. However, we cannot rule out the additional presence of small adsorbate molecules (such as water) within these structures.

The network shown in panels a and b of Figure 3 comprises double rings of uracil, linked by parallel pairs of PTCI molecules arranged in a cross-like manner. We will refer to this structure as the “double-cross”. The uracil double-rings are slightly elliptical in shape and show distinct similarities to the chain structure of Figure 2 since, in both of these structures, neighboring uracil molecules from each ring are aligned radially. However, the outer ring of the double-cross structure appears to be missing four uracil molecules (one in each quadrant), the

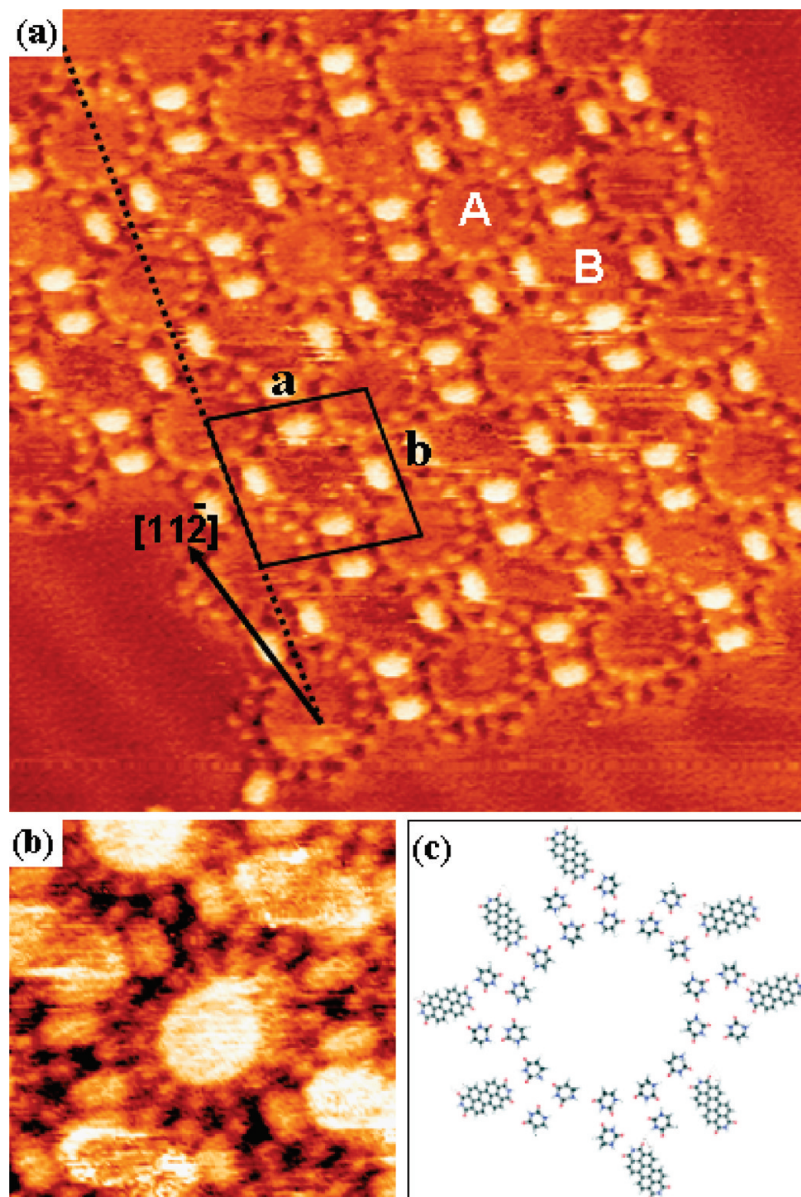


Figure 3. (a) A region of the double-cross uracil-PTCDI network ($V_s = -1.0$ V, $I_t = 0.05$ nA, 27.1 nm \times 27.1 nm). The unit cell is indicated by a black parallelogram, while a dotted black line highlights the $\sim 9^\circ$ rotation of this structure with respect to the [11 $\bar{2}$] directions of the Au(111) surface. Two pore types are identified, labeled A and B. (b) A higher resolution image of the double-cross structure ($V_s = -1.5$ V, $I_t = 0.05$ nA, 8.6 nm \times 8.6 nm). (c) Proposed molecular arrangement of the double-cross structure.

positions of which are instead occupied by the ends of four PTCDI molecules. The other ends of these PTCDI link to the outer edge of neighboring uracil double-rings. The different arrangements of uracil at either end of the PTCDI molecules lead to one of the PTCDI protruding further out of the ring than its parallel near-neighbor, and give rise to chirality. The double-cross motif has two rotational axes and its unit cell is a parallelogram. This structure is therefore of the p2 chiral plane group (as described in the Two-Dimensional Structural Database).²⁶

The double-cross network has two different porous sites. The pore marked A in Figure 3a is outlined by uracil molecules and is circular. In addition, a rectangular pore, framed by PTCDI molecules in the corners, is also formed (labeled B in Figure 3a). A network possessing two different pore shapes is particularly interesting since it opens up the possibility of generating different packing arrangements of guest molecules in close proximity to each other. The double-cross structure is

rotated by $9(\pm 1)^\circ$ from the [11 $\bar{2}$] direction of the Au(111) surface. A preferred crystallographic orientational relationship between the network and the Au(111) surface demonstrates the anisotropic nature of the substrate. This effect is not unexpected as it is frequently observed for similar hydrogen-bonded networks.^{6–8,15,19,27,28} This structure's unit cell has dimensions of $a = 5.1 \pm 0.2$ nm, $b = 4.7 \pm 0.2$ nm, and $\theta = 81(\pm 1)^\circ$ and contains 24 uracil and 4 PTCDI molecules.

Our high-resolution images allow us to propose a potential arrangement of the uracil and PTCDI molecules in the double-cross network. Although it is not possible to determine the orientation of the uracil molecules directly from our STM images, it is probable that an arrangement that maximizes the number of O \cdots H–N bonds is formed. We therefore envisage that the arrangement shown in Figure 3c is likely (a more detailed schematic that indicates bonding is given in Figure S1, Supporting Information). In our proposed molecular arrangement, the inner ring comprises 14 uracil molecules and is slightly

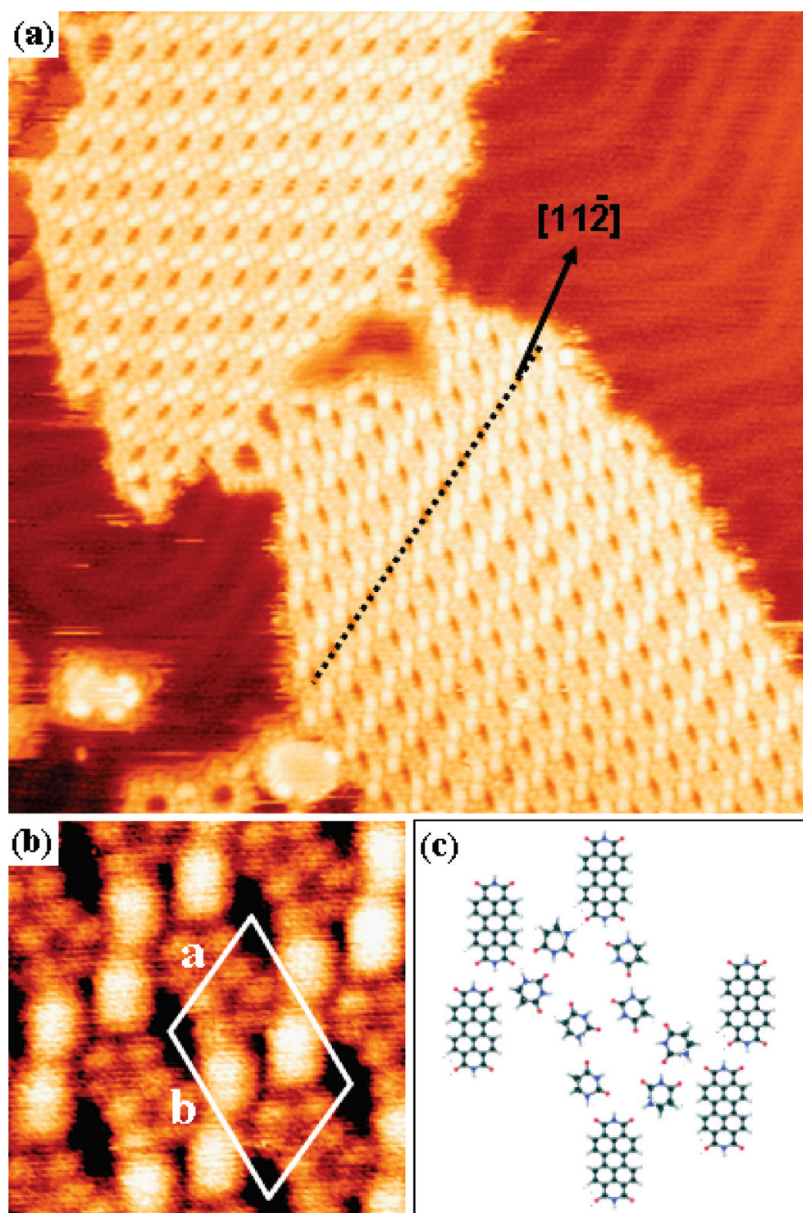


Figure 4. (a) An image showing two regions of the uracil-PTCDI staircase structure ($V_s = -1.5$ V, $I_t = 0.05$ nA, 60.6 nm \times 60.6 nm). A dotted black line runs parallel to the translation vector. This network is oriented $7(\pm 1)$ ° from the [112] directions of the Au(111) surface. (b) A more detailed image of the staircase network, in which the unit cell is indicated ($V_s = -1.5$ V, $I_t = 0.10$ nA, 7.3 nm \times 7.3 nm). (c) Our proposed model of the staircase structure.

elliptical in shape, consistent with our experimental observations. The inner uracil molecules are of one chirality, while the outer uracil molecules are of the opposite chirality. Although this locally leads to a slight imbalance of the ratio of the two uracil chiralities, this is globally relieved by the formation of both complementary chiral structures, as we have observed.

The double-cross structure coexists with a different porous network, which is shown in Figure 4a,b. This comprises rows of end-to-end PTCDI pairs sandwiching two overlapping pentagonal uracil clusters. We denote this structure the “staircase” network. The unit cell contains 8 uracil and 2 PTCDI molecules, and has dimensions $a = 2.4 \pm 0.2$ nm, $b = 3.5 \pm 0.2$ nm, and $\theta = 63(\pm 2)$ °. We propose a possible molecular structure of the staircase network (Figure 4c, also Figure S2 in the Supporting Information), again based on our experimental observations and the requirement to maximize the possible number of hydrogen bonds. This arrangement contains equal numbers of the two chiralities of uracil. Similarities within this

network are observed with the monomer structures, such as the pentagonal uracil features (Figure 2b) and the end-on binding of PTCDI molecules.¹⁶ In general, domains of the staircase network are larger than those of the double-cross structure, with average domain areas of 3800 nm 2 (standard deviation of 2200 nm 2) and 440 nm 2 (standard deviation of 400 nm 2), respectively. Presumably this difference arises from the larger intricacy of the latter. The smaller double-cross fragments, however, are more numerous than the staircase domains, although still only cover 7–13% of the total surface area (we observe that the staircase network covers 11–37% of the Au(111) surface).

We now turn to combinations of uracil and melamine, from which we have successfully generated two different networks which cover most of the surface (Figure 5). Small fragments of these networks are formed after codeposition at room temperature, but after annealing to ~ 90 °C for ~ 12 h these structures grow in size and number, while single-component melamine and uracil regions are no longer observed. Both networks look

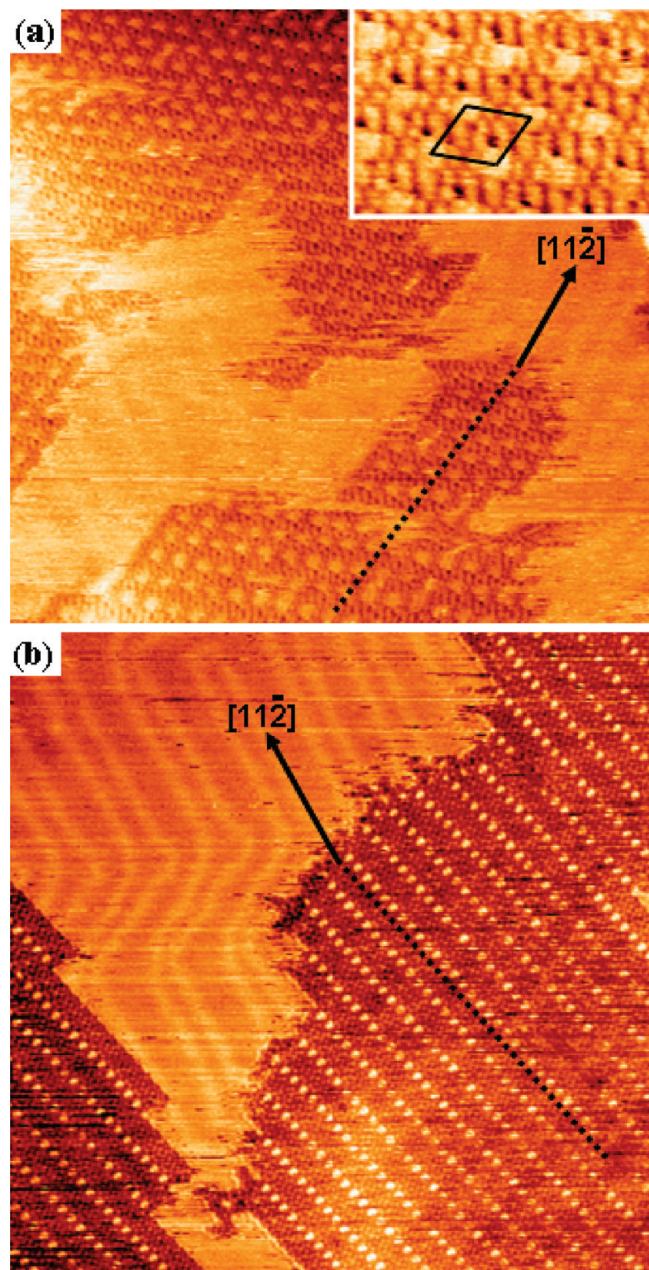


Figure 5. (a) A region of a supramolecular network of melamine and uracil ($V_s = +1.0$ V, $I_t = 0.07$ nA, 61.4 nm \times 61.4 nm). A higher resolution image is shown in the inset, in which the unit cell is marked ($V_s = +1.0$ V, $I_t = 0.07$ nA, 17.0 nm \times 17.0 nm). (c) A second structure of melamine-uracil ($V_s = +1.0$ V, $I_t = 0.07$ nA, 66.0 nm \times 66.0 nm). Dotted lines indicate the direction of the translation vectors for each network, while the $[11\bar{2}]$ direction of the Au(111) surface is also indicated in each image.

very different from those of pure uracil (Figure 2) and pure melamine²⁹ on Au(111). We therefore attribute these structures to mixtures of melamine and uracil. The most commonly observed network, shown in Figure 5a, is rotated by $7(\pm 1)^\circ$ with respect to the $[11\bar{2}]$ directions of the Au(111) surface. The unit cell is indicated in the inset and has dimensions $a = b = 2.3 \pm 0.2$ nm and $\theta = 115(\pm 1)^\circ$. In contrast, the unit cell of the network shown in Figure 5b is more elongated, with $a = 2.9 \pm 0.2$ nm, $b = 1.2 \pm 0.2$ nm, and $\theta = 98(\pm 1)^\circ$. It has not been possible to distinguish between the uracil and melamine molecules in these images, owing to their similar sizes, and so we refrain from proposing a structural model for either network. However, we suggest that both supramolecular networks are

predominantly stabilized by hydrogen bonds, in a similar manner to three-dimensional melamine-uracil crystals³⁰ and their monomer two-dimensional counterparts.^{19,20,29}

We have established that a range of supramolecular structures can be constructed from uracil-PTCDI and uracil-melamine, while melamine and PTCDI are well-known to form a range of porous networks on Au(111).^{6–8,15,16} We now report on ternary mixtures of all three species. Combining three molecules with the potential for hydrogen bonding is an attractive approach to generating more intricate and even larger supramolecular networks. Figure 6 shows the highly ordered porous structure formed from 0.1–0.3 ML of melamine, 0.2–0.3 ML of uracil, and 0.3–0.4 ML of PTCDI after annealing to ~ 120 °C for 10–12 h. Patches of this structure cover on average 24–38% of the surface, with only close-packed PTCDI regions otherwise observed. When the three components are mixed and annealed at a lower temperature of ~ 100 °C for ~ 2 h, small fragments of the bimolecular networks are often found. Examples of such are given in Figure 7. In Figure 7a, small regions of a parallelogram structure formed by PTCDI and melamine⁶ are seen, as highlighted by white arrows. Combinations of PTCDI and uracil are also observed, for example, as shown in Figure 7b, where the double-cross structure is formed. However, after subsequent annealing to ~ 130 °C, we do not observe any of the possible binary structures, nor any single phase uracil or melamine regions (any excess of the latter two are likely to have sublimed from the surface during annealing). The formation of one ternary structure, as opposed to the several possible bimolecular structures, demonstrates the capacity of hydrogen bonding to drive the formation of highly complex structures.

As can be seen from Figure 6a,b, the network formed from PTCDI, melamine, and uracil has large hexagonal pores each of which are surrounded by six smaller triangular voids. We name this structure the “star” network due to its similarity to the Star of David. Chevron-shaped clusters of three uracil and/or melamine protrude from the apex points of each hexagon giving rise to chirality. Networks of the two complementary chiralities are observed (one of each is shown in panels a and b of Figure 6). The intricate unit cell of the star structure, which is marked in Figure 6a, has dimensions $a = b = 6.6 \pm 0.3$ nm and $\theta = 121(\pm 2)^\circ$ and contains 33 molecules. The average area of the star domains is 1200 nm² (standard deviation of 1000 nm²).

The orientation of the star network with respect to the Au(111) surface can be inferred from Figure 6c. It is likely that this image has been acquired with an adsorbate on the tip, causing the molecules to appear darker than the Au substrate but enhancing the resolution of the surface reconstruction. For comparison, an image of the same region obtained after applying a brief electrical pulse to the tip to remove the adsorbate is provided in the inset. Two regions of opposite chirality are shown in Figure 6c; more detailed images (not shown) reveal that region A is the same as Figure 6a, while region B is of the same chirality as the structure shown in Figure 6b. Although both unit cells are offset by $9(\pm 1)^\circ$ with respect to the Au(111) $[11\bar{2}]$ directions, the local chirality of the network appears to define the orientation of each unit cell with respect to the substrate. We note that in all cases the hexagonal rings are aligned parallel to $[11\bar{2}]$ directions of the Au(111) surface, i.e., they are rotated by $9(\pm 1)^\circ$ from the translation vectors, as indicated by the dotted line in Figure 6a.

Although we are unable to confidently distinguish between uracil and melamine in the star structure, we look to similarities with other known binary structures to enable us to propose a

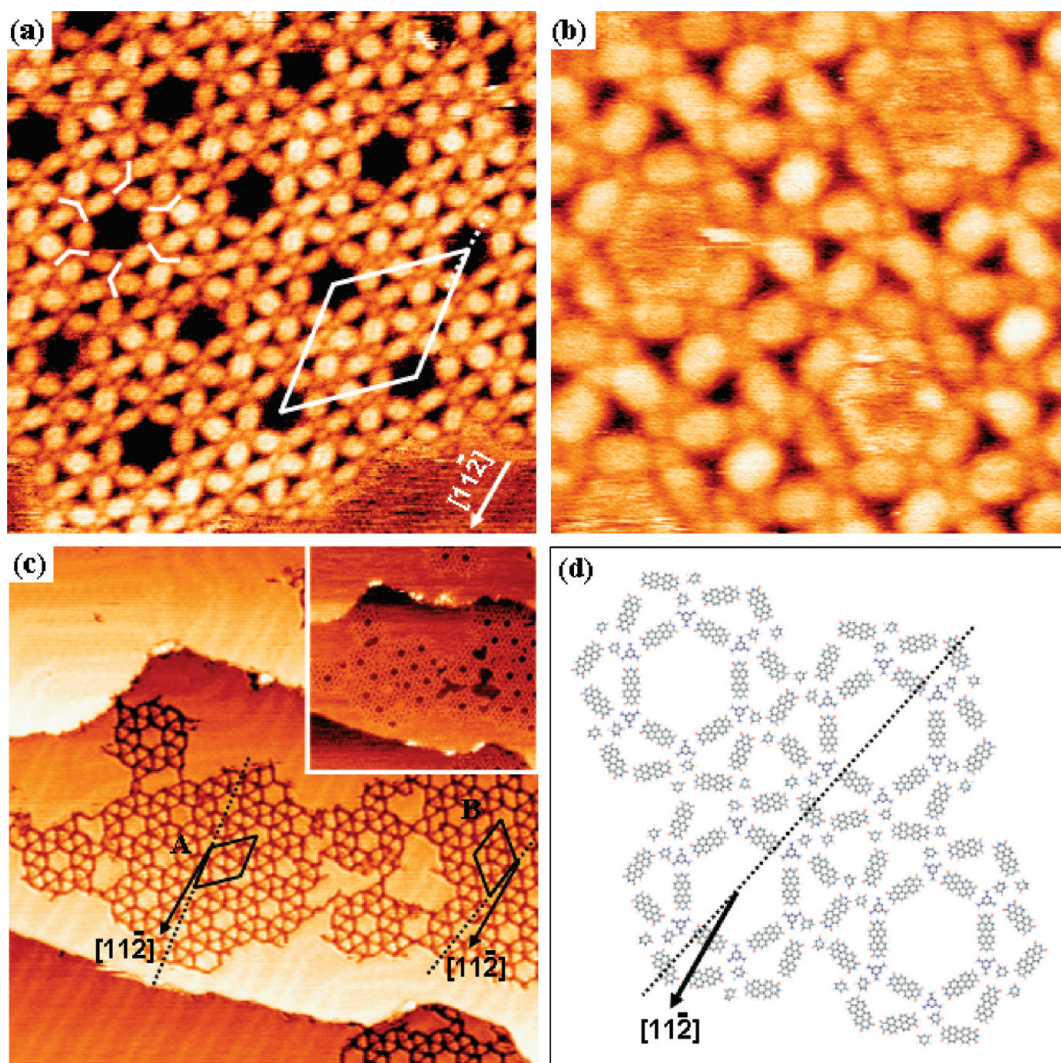


Figure 6. (a) The star network, composed of melamine, uracil, and PTCDI ($V_s = -2.0$ V, $I_t = 0.04$ nA, 27.5 nm \times 27.5 nm). White chevrons overlap the cluster of three molecules extending from the hexagonal apexes, which give rise to chirality. The unit cell is indicated by a white solid parallelogram, while a dashed line depicts a symmetry axis of a hexagonal pore. (b) A more detailed image of the star network ($V_s = -2.0$ V, $I_t = 0.04$ nA, 12.8 nm \times 12.8 nm). This region is of opposite chirality to that in panel a. (c) An image of two regions (marked A and B) of the star network, in which the Au(111) reconstruction can be resolved ($V_s = -2.0$ V, $I_t = 0.04$ nA, 77.4 nm \times 77.4 nm). The unit cells and translation directions of each domain are indicated by black parallelograms and dotted lines, respectively. This image displays an unusual contrast effect most likely due to an adsorbate on the tip; an image of the same region of more standard appearance is shown in the inset ($V_s = -2.0$ V, $I_t = 0.04$ nA, 77.1 nm \times 77.1 nm). (d) A possible arrangement of uracil, melamine, and PTCDI molecules within the star structure. This represents a region with the same chirality as in image b and region B of image c. The stacking and Au(111) [112] directions are indicated by a dotted line and solid arrow, respectively.

potential molecular arrangement. The central hexagon is identical in orientation with respect to the Au(111) surface, size, and shape to hexagonal rings of PTCDI-melamine formed on Au(111),^{6,7} and so we attribute this part of the structure to an analogous arrangement of PTCDI and melamine. However, the star network has not been previously observed for the well-characterized PTCDI-melamine system, and so it is unlikely to be composed solely of PTCDI and melamine. Instead, we propose that the triangular apexes, which are not known features of PTCDI-melamine structures, contain uracil. We therefore deduce that the star structure is the first ternary porous hydrogen-bonded network to be reported. We propose a molecular arrangement shown in Figure 6d, which has been constructed to maximize the number of N \cdots H–N and O \cdots H–N bonds formed. This arrangement contains 15 PTCDI, 6 melamine, and 12 uracil (6 of each chirality) per unit cell. A more detailed schematic of this arrangement, which indicates the hydrogen bonds formed, is given in Figure S3 (Supporting Information). In this arrangement, all N lone pairs form N \cdots H–N bonds,

while all N–H groups form either O \cdots H–N or N \cdots H–N bonds (i.e., none of the weaker N \cdots H–C bonds are possible). As with the other structures proposed, detailed theoretical simulations would be required to verify the thermodynamic stability of this structure and elucidate whether water molecules are bound to the networks. However, a rough guide to the relative stabilities of the possible binary and ternary structures can be obtained by comparing the bonding energies per unit area. Assuming bond energies of 8 and 13 kJ/mol for O \cdots HN and N \cdots HN, respectively, we find the ternary (star) structure to have the largest bond energy per unit area (21.7 kJ mol $^{-1}$ nm $^{-2}$), while the corresponding energies of binary PTCDI-uracil (double-cross and staircase) and PTCDI-melamine (honeycomb⁶) networks are 19.0 , 19.3 , and 16.4 kJ mol $^{-1}$ nm $^{-2}$, respectively. Hence, to a first approximation the star network is expected to be the most stable, in agreement with our experimental observations of the formation of a single ternary structure.

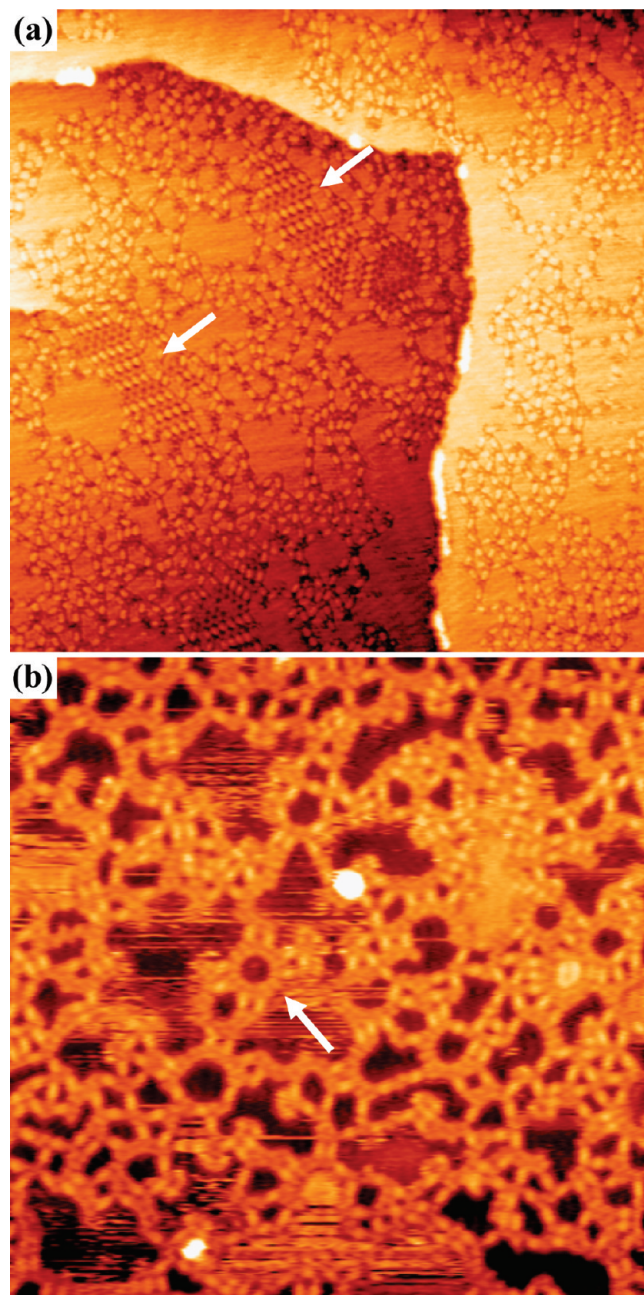


Figure 7. Mixtures of uracil, melamine, and PTCDI formed after annealing to $\sim 100\text{ }^{\circ}\text{C}$ for 2 h (both images obtained at room temperature). (a) An image in which many disordered regions can be observed, although small fragments of PTCDI-melamine in the parallelogram structure are highlighted by white arrows ($V_s = -1.5\text{ V}$, $I_t = 0.04\text{ nA}$, $79.9\text{ nm} \times 79.9\text{ nm}$). (b) A different region of the same sample that is again largely disordered ($V_s = -1.5\text{ V}$, $I_t = 0.04\text{ nA}$, $49.8\text{ nm} \times 49.8\text{ nm}$). A small fragment of the double-cross PTCDI-uracil structure is indicated by a white arrow.

The star structure has one main pore and eight smaller voids per unit cell which could be used to trap guest molecules, such as fullerenes. We have sublimed C_{82} onto the structure and have observed that they occupy both classes of site, as shown in Figure 8. Between three and six C_{82} molecules are situated within the hexagonal pores; the distribution of occupancy number is consistent with that of C_{84} in the hexagonal PTCDI-melamine structure.⁹ In addition, single C_{82} can be trapped in the triangular voids. This confirms that the intricacy of the star

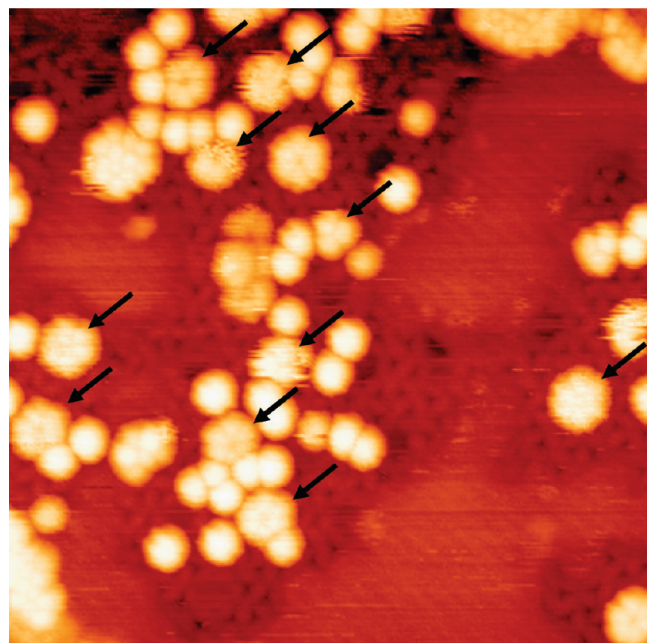


Figure 8. The arrangement of C_{82} molecules after deposition onto the star network ($V_s = -2.0\text{ V}$, $I_t = 0.04\text{ nA}$, $53.5\text{ nm} \times 53.3\text{ nm}$). Small clusters of C_{82} are observed within the hexagonal pores (examples of which are indicated by black arrows), while individual C_{82} occupy the smaller triangular pores.

structure gives rise to multiple absorption sites for host molecules and can be used to produce complex ordering of fullerenes.

Conclusions

In conclusion, we have formed a variety of two-dimensional porous networks from combinations of uracil, melamine, and PTCDI. Two different supramolecular structures have been produced from uracil and PTCDI, both of which contain features observed in pure uracil double-chains. One of these structures, which we have termed the double-cross, has a unit cell of 28 molecules, while the staircase structure contains 10 molecules per unit cell. In addition, melamine and uracil have been shown to form two different structures. It therefore seems likely that many other bimolecular networks, with a range of pore shapes and sizes, could be generated by combinations of other nucleic bases with either PTCDI or melamine.

Through the combination of PTCDI, uracil, and melamine, we have produced a highly intricate network. The somewhat surprising formation of a three-component network, rather than phase segregated binary regions, opens up the possibility of designing a range of new, complex structures. This could be achieved through the use of other nucleic bases, small cyclic molecules (such as trimesic acid) or perylene derivatives, or through chemical functionalization of the molecular components.³¹ Such networks could then be used to generate a variety of complicated arrangements of guest molecules.

Acknowledgment. The authors thank the EPSRC for funding (EP/D048761/1 and GR/S15808/01). We thank Dr. K. Porfyrikis for provision of C_{82} and C. Spencer (JEOL UK) for technical support.

Supporting Information Available: Schematics showing the possible hydrogen bond formed within the PTCDI-uracil

and PTCDI-uracil-melamine networks. This material is available free of charge via the Internet at <http://pubs.acs.org>.

References and Notes

- (1) Kudernac, T.; Lei, S.; Elemans, J. A. A. W.; De Feyter, S. *Chem. Soc. Rev.* **2009**, *38*, 402–421.
- (2) Theobald, J. A.; Oxtoby, N. S.; Phillips, M. A.; Champness, N. R.; Beton, P. H. *Nature* **2003**, *424*, 1029–1031.
- (3) Zhang, H. L.; Chen, W.; Huang, H.; Chen, L.; Wee, A. T. S. *J. Am. Chem. Soc.* **2008**, *130*, 2720–2721.
- (4) Kiebele, A.; Bonifazi, D.; Cheng, F.; Stohr, M.; Diederich, F.; Jung, T.; Spillmann, H. *Chem. Phys. Chem.* **2006**, *7*, 1462–1470.
- (5) Li, M.; Deng, K.; Lei, S.-B.; Yang, Y.-L.; Wang, T.-S.; Shen, Y.-T.; Wang, C.-R.; Zeng, Q.-D.; Wang, C. *Angew. Chem.* **2008**, *120*, 6819–6823.
- (6) Silly, F.; Shaw, A. Q.; Porfyrikis, K.; Briggs, G. A. D.; Castell, M. R. *Appl. Phys. Lett.* **2007**, *91*, 253109.
- (7) Perdigao, L. M. A.; Perkins, E. W.; Ma, J.; Staniec, P. A.; Rogers, B. L.; Champness, N. R.; Beton, P. H. *J. Phys. Chem. B* **2006**, *110*, 12539–12542.
- (8) Staniec, P. A.; Perdigao, L. M. A.; Saywell, A.; Champness, N. R.; Beton, P. H. *Chem. Phys. Chem.* **2007**, *8*, 2177–2181.
- (9) Theobald, J. A.; Oxtoby, N. S.; Champness, N. R.; Beton, P. H.; Dennis, T. J. S. *Langmuir* **2005**, *21*, 2038–2041.
- (10) Otero, R.; Schock, M.; Molina, L. M.; Loegsgaard, E.; Stensgaard, I.; Hammer, B.; Besenbacher, F. *Angew. Chem., Int. Ed.* **2005**, *44*, 2270–2275.
- (11) Sivakova, S.; Rowan, S. J. *Chem. Soc. Rev.* **2005**, *34*, 9–21.
- (12) Griessl, S.; Lackinger, M.; Edelwirth, M.; Hietschold, M.; Heckl, W. M. *Single Mol.* **2002**, *3*, 25–31.
- (13) Pawin, G.; Wong, K. L.; Kwon, K.-Y.; Bartels, L. *Science* **2006**, *313*, 961–962.
- (14) Kong, X.-H.; Deng, K.; Yang, Y.-L.; Zeng, Q.-D.; Wang, C. *J. Phys. Chem. C* **2007**, *111*, 17382–17387.
- (15) Silly, F.; Shaw, A. Q.; Briggs, G. A. D.; Castell, M. R. *Appl. Phys. Lett.* **2008**, *92*, 023102.
- (16) Silly, F.; Shaw, A. Q.; Castell, M. R.; Briggs, G. A. D. *Chem. Commun.* **2008**, 1907–1909.
- (17) Lei, S.; Surin, M.; Tahara, K.; Adisojoso, J.; Lazzaroni, R.; Tobe, Y.; De Feyter, S. *Nano Lett.* **2008**, *8*, 2541–2546.
- (18) Li, Y.; Ma, Z.; Deng, K.; Lei, S.; Zheng, Q.; Fan, X.; De Feyter, S.; Juang, W.; Wang, C. *Chem.—Eur. J.* **2009**, *15*, 5418–5423.
- (19) Dretschkow, Th.; Dakkouri, A. S.; Wandlowski, Th. *Langmuir* **1997**, *13*, 2843–2856.
- (20) Sowerby, S. J.; Stockwell, P. A.; Heckl, W. M.; Petersen, G. B. *Origins Life Evol. Biospheres* **2000**, *30*, 81–99.
- (21) Parry, G. S. *Acta Crystallogr.* **1954**, *7*, 313–320.
- (22) Horcas, I.; Fernandez, R.; Gomez-Rodriguez, J. M.; Colchero, J.; Gomez-Herrero, J.; Baro, A. M. *Rev. Sci. Instrum.* **2007**, *78*, 013705.
- (23) Kelly, R. E. A.; Lukas, M.; Kantorovich, L. N.; Otero, R.; Xu, W.; Mura, M.; Laegsgaard, E.; Stensgaard, I.; Besenbacher, F. *J. Chem. Phys.* **2003**, *129*, 184707.
- (24) Otero, R.; Lukas, M.; Kelly, R. E. A.; Xu, W.; Laegsgaard, E.; Stensgaard, I.; Kantorovich, L. N.; Besenbacher, F. *Science* **2008**, *319*, 312–315.
- (25) Xu, W.; Kelly, R. E. A.; Otero, R.; Schock, M.; Laegsgaard, E.; Stensgaard, I.; Kantorovich, L. N.; Besenbacher, F. *Small* **2007**, *12*, 2011–2014.
- (26) Plass, K. E.; Grzesiak, A. L.; Matzger, A. J. *Acc. Chem. Res.* **2007**, *40*, 287–293.
- (27) Zhang, H.-M.; Xie, Z.-X.; Long, L.-S.; Zhong, H.-P.; Zhao, W.; Mao, B.-W.; Xu, X.; Zhen, L.-S. *J. Phys. Chem. C* **2008**, *112*, 4209–4218.
- (28) Su, G.-J.; Zhang, H.-M.; Wan, L.-J.; Bai, C.-L.; Wandlowski, T. *J. Phys. Chem. B* **2004**, *108*, 1931–1937.
- (29) Silly, F.; Shaw, A. Q.; Castell, M. R.; Briggs, G. A. D.; Mura, M.; Martsinovich, N.; Kantorovich, L. *J. Phys. Chem. C* **2008**, *112*, 11476–11480.
- (30) Thomas, R.; Kulkarni, G. U. *Beilstein J. Org. Chem.* **2007**, *3*, 17.
- (31) Perdigao, L. M. A.; Saywell, A.; Fontes, G. N.; Staniec, P. A.; Goretzki, G.; Phillips, A. G.; Champness, N. R.; Beton, P. H. *Chem.—Eur. J.* **2008**, *14*, 7600–7607.

JP9113249